



The radial pressure gradient for turbulent flow in smooth pipes
by Charles Willis Greene

A thesis submitted to the Graduate Faculty in partial fulfillment of the requirements for the degree of
MASTER OF SCIENCE in Aerospace and Mechanical Engineering

Montana State University

© Copyright by Charles Willis Greene (1971)

Abstract:

An expression predicting a radial pressure gradient in turbulent smooth tube flow was derived. The radial pressure gradient for turbulent flow in smooth tubes was then measured experimentally for a range of Reynolds numbers from 57,000 to 484,000.

The results of the measurements show poor agreement with the predicted radial pressure gradient. The measured values were from four to thirteen times greater than the predicted values and indicate that the probe used did not measure the quantity which was, expected.

Statement of Permission to Copy

In presenting this thesis in partial fulfillment of the requirements for an advanced degree at Montana State University, I agree that the Library shall make it freely available for inspection. I further agree that permission for extensive copying of this thesis for scholarly purposes may be granted by my major professor, or, in his absence, by the Director of Libraries. It is understood that any copying or publication of this thesis for financial gain shall not be allowed without my written permission.

Signature

Charles W. Greene

Date

Dec. 15, 1970

THE RADIAL PRESSURE GRADIENT FOR
TURBULENT FLOW IN SMOOTH PIPES

by

CHARLES WILLIS GREENE

A thesis submitted to the Graduate Faculty in partial
fulfillment of the requirements for the degree

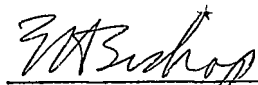
of


MASTER OF SCIENCE

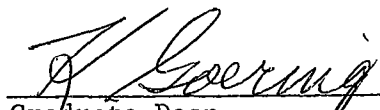
in

Aerospace and Mechanical Engineering

Approved:


Head, Major Department


Chairman, Examining Committee


Graduate Dean

MONTANA STATE UNIVERSITY
Bozeman, Montana

March, 1971

ACKNOWLEDGMENT

The author wishes to extend his sincere appreciation to Dr. Harry Townes under whose guidance this study was possible. Special thanks also are given to Dr. Ralph E. Powe whose assistance is deeply appreciated. Finally, the author's gratitude is also extended to Mr. Gordon Williamson for his skill at constructing the various probes used in this investigation.

TABLE OF CONTENTS

<u>Chapter</u>	<u>Page</u>
VITA	ii
ACKNOWLEDGMENT	iii
LIST OF FIGURES	v
NOMENCLATURE	vi
ABSTRACT	viii
I. INTRODUCTION	1
II. ANALYTICAL DEVELOPMENT	2
III. LITERATURE REVIEW	9
IV. EXPERIMENTAL SYSTEM	12
Apparatus	12
Procedure	17
V. EXPERIMENTAL RESULTS	21
VI. CONCLUSION AND RECOMMENDATIONS	30
APPENDIX I	31
LITERATURE CITED	33

LIST OF FIGURES

<u>Figure</u>		<u>Page</u>
1	Mean Velocity Distribution With Fluctuating Components	4
2	Axial Section of Pipe at an Arbitrarily Selected Zero Position	7
3	Schematic of Experimental System	13
4	Final Probe Design	15
5	Normal Stress Differences at $Re = 57,000$	24
6	Normal Stress Differences at $Re = 162,000$	25
7	Normal Stress Differences at $Re = 292,000$	26
8	Normal Stress Differences at $Re = 484,000$	27
9	Dimensionless Normal Stress Difference Between Pipe Wall and Center Line as a Function of Reynolds Number	28

NOMENCLATURE

<u>Symbol</u>	<u>Description</u>
D	Pipe diameter
P	Mean Pressure at any point in pipe
\bar{P}	Time average of mean pressure
r	Radial Coordinate
R	Pipe radius
Re	Reynolds number = $\frac{U_{avg} D}{\nu}$
T	Temperature
u^*	Shear Velocity $(\tau_o/\rho)^{1/2}$
U	Mean velocity in axial direction
U_{avg}	Bulk mean velocity
U_{max}	Centerline mean velocity
u	Instantaneous value of fluctuating velocity in axial direction
\bar{u}	Time average value of instantaneous fluctuating velocity in axial direction
V	Mean velocity in radial coordinate direction
v	Instantaneous value of fluctuating velocity in radial direction
\bar{v}	Time average value of instantaneous fluctuating velocity in radial direction
W	Mean velocity in angular coordinate direction
w	Instantaneous value of fluctuating velocity in

<u>Symbol</u>	<u>Description</u>
	angular direction
\bar{w}	Time average value of instantaneous fluctuating velocity in angular direction
z	Axial Coordinate

<u>Greek Symbols</u>	<u>Description</u>
θ	Angular coordinate
ρ	Air density
ν	Kinematic viscosity
τ	Turbulent shear stress
τ_o	Wall shear stress
$\tau_{\theta\theta}$	Normal shear stress in the angular (θ) direction
κ	Bulk viscosity
∇	$\frac{\partial}{\partial r} + \frac{1}{r} \frac{\partial}{\partial r} + \frac{1}{r} \frac{\partial}{\partial \theta} + \frac{\partial}{\partial z}$
∇^2	$\frac{\partial^2}{\partial r^2} + \frac{1}{r} \frac{\partial}{\partial r} + \frac{1}{r^2} \frac{\partial^2}{\partial \theta^2} + \frac{\partial^2}{\partial z^2}$

<u>Subscripts</u>	<u>Description</u>
C	Refers to pipe centerline
W	Refers to pipe wall

ABSTRACT

An expression predicting a radial pressure gradient in turbulent smooth tube flow was derived. The radial pressure gradient for turbulent flow in smooth tubes was then measured experimentally for a range of Reynolds numbers from 57,000 to 484,000.

The results of the measurements show poor agreement with the predicted radial pressure gradient. The measured values were from four to thirteen times greater than the predicted values and indicate that the probe used did not measure the quantity which was expected.

CHAPTER I

INTRODUCTION

Turbulent flow in smooth tubes and over smooth boundaries has been studied quite extensively. As a result, theoretical studies, experimental data and semi-empirical theory have been developed which agree reasonably well. The theoretical expressions for turbulent flow in smooth tubes have also led to the development of an expression which predicts a radial pressure gradient in turbulent smooth tube flow. However, no experimental work has been done to verify the existence of this pressure gradient. Heretofore, this predicted radial pressure gradient has been considered negligible.

The purpose of this study was to experimentally measure the predicted radial pressure gradient in smooth tubes and to compare the measured values with the predicted values.

CHAPTER II

ANALYTICAL DEVELOPMENT

For turbulent pipe flow, a radial pressure gradient can be shown theoretically to exist. The Reynolds equations for incompressible flow in the three coordinate directions

$$U \frac{\partial U}{\partial z} + V \frac{\partial U}{\partial r} + \frac{W}{r} \frac{\partial U}{\partial \theta} = - \frac{1}{\rho} \frac{\partial P}{\partial z} - \left(\frac{\partial \overline{u^2}}{\partial z} + \frac{1}{r} \frac{\partial (r \overline{uv})}{\partial r} + \frac{1}{r} \frac{\partial (\overline{uw})}{\partial \theta} \right) + \nu \nabla^2 U, \quad (2.1)$$

$$U \frac{\partial V}{\partial z} + V \frac{\partial V}{\partial r} + \frac{W}{r} \frac{\partial V}{\partial \theta} - \frac{W^2}{r} = - \frac{1}{\rho} \frac{\partial P}{\partial r} - \left(\frac{\partial \overline{uv}}{\partial z} + \frac{1}{r} \frac{\partial (r \overline{v^2})}{\partial r} + \frac{1}{r} \frac{\partial (\overline{vw})}{\partial \theta} - \frac{\overline{w^2}}{r} \right) + \nu \left(\nabla^2 V - \frac{V}{r^2} - \frac{2}{r^2} \frac{\partial W}{\partial \theta} \right), \quad (2.2)$$

and

$$U \frac{\partial W}{\partial z} + V \frac{\partial W}{\partial r} + \frac{W}{r} \frac{\partial W}{\partial \theta} + \frac{VW}{r} = - \frac{1}{\rho} \frac{\partial P}{\partial \theta} - \left(\frac{\partial (\overline{uw})}{\partial z} + \frac{\partial (\overline{vw})}{\partial r} + \frac{1}{r} \frac{\partial (\overline{w^2})}{\partial \theta} - \frac{2\overline{vw}}{r} \right) + \nu \left(\nabla^2 W + \frac{2}{r^2} \frac{\partial W}{\partial \theta} - \frac{W}{r^2} \right). \quad (2.3)$$

are obtained from the Navier Stokes equations by introducing the fluctuating velocity terms and time averaging each equation. The development of these expressions (2.1, 2.2, and 2.3) may be found in

such references as Hinze [1]¹ and Pai [4]. For the case of axially symmetric fully-developed pipe flow, the mean velocity components V and W are zero, all partial derivatives with respect to θ are zero because of symmetry and all velocity terms are independent of the axial component z . Therefore, the mean axial velocity component is a function of r only and the Reynolds equations reduce to

$$\frac{\partial(\overline{v^2})}{\partial r} + \frac{(\overline{v^2} - \overline{w^2})}{r} = -\frac{1}{\rho} \frac{\partial \overline{P}}{\partial r} \quad (2.4)$$

$$\frac{d(\overline{vw})}{dr} + \frac{2(\overline{vw})}{r} = 0 \quad (2.5)$$

and

$$\frac{d(\overline{vu})}{dr} + \frac{\overline{vu}}{r} = -\frac{1}{\rho} \frac{\partial \overline{P}}{\partial z} + \nu \left[\frac{d^2 U}{dr^2} + \frac{1}{r} \frac{dU}{dr} \right] \quad (2.6)$$

These equations can be simplified further by means of the following considerations. Figure 1 is a sketch showing the fluctuating velocity components and mean velocity profile in turbulent pipe flow. For any given point in the pipe, a fluctuation in the w component will result in no fluctuation in the u or v components. Therefore, it may be inferred that there can be no correlation of the v and w velocity fluctuations. If $\overline{vw} = 0$ then equation 2.5 is satisfied identically

¹Numbers in brackets refer to literature cited.

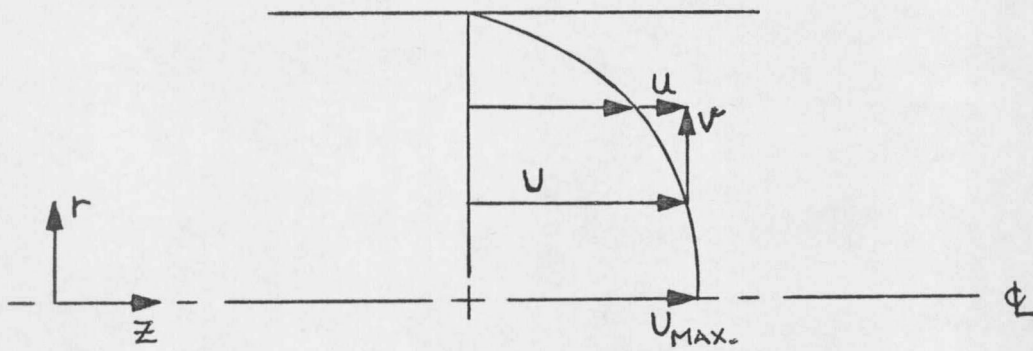


FIGURE 1. Mean Velocity Distribution With Fluctuating Components.

and of no further use.

Equation (2.4) may be rewritten as

$$-\frac{1}{\rho} \frac{\partial \bar{P}}{\partial r} = \frac{\partial \bar{v}^2}{\partial r} + \frac{(\bar{v}^2 - \bar{w}^2)}{r} \quad (2.7)$$

By integrating equation (2.7) with respect to r , the resulting equation is

$$\int_0^r \frac{\partial \bar{P}}{\partial r} dr = -\rho \int_0^r \left[\frac{\partial \bar{v}^2}{\partial r} + \frac{\bar{v}^2 - \bar{w}^2}{r} \right] dr \quad (2.8)$$

or

$$\bar{P} - \bar{P}_C = -\rho \left[(\bar{v}^2 - \bar{v}_C^2) + \int_0^r \frac{\bar{v}^2 - \bar{w}^2}{r} dr \right] + f(z) \quad (2.9)$$

where $f(z)$ is an unknown function of z .

The terms within the integral of equation (2.9) are functions only of the radial position r . Since the terms within the brackets of equation (2.9) are functions of r only, and since

$$\frac{\partial \bar{P}}{\partial z} = C \quad (2.10)$$

for fully developed flow then $f(z)$ must be

$$f(z) = C z \quad (2.11)$$

which can be taken as zero for an arbitrary axial position as in Figure 2.

Equation (2.9) then becomes

$$\bar{P} - \bar{P}_C = -\rho \left[(\bar{v}^2 - \bar{v}_C^2) + \int_0^r \frac{\bar{v}^2 - \bar{w}^2}{r} dr \right] \quad (2.12)$$

Equation (2.12) is then an equation for the mean static pressure of the fluid at any radial position minus the mean static pressure at the centerline. A similar expression for the mean static pressure at the wall minus the mean static pressure of the fluid at any radial position may be found by integrating equation (2.7) with respect to r again only between the limits of r and R . Following the same procedure as used in deriving equation (2.12) gives

$$\bar{P}_W - P = \rho \bar{v}^2 - \rho \int_r^R \frac{\bar{v}^2 - \bar{w}^2}{r} dr \quad (2.13)$$

Finally, by evaluating equation (2.13) at the centerline or by evaluating equation (2.12) at the wall, the theoretical expression for mean static pressure at the wall minus mean static pressure at the centerline may be found and is

$$\bar{P}_W - \bar{P}_C = \rho \bar{v}_C^2 - \rho \int_0^R \frac{\bar{v}^2(r) - \bar{w}^2(r)}{r} dr \quad (2.14)$$

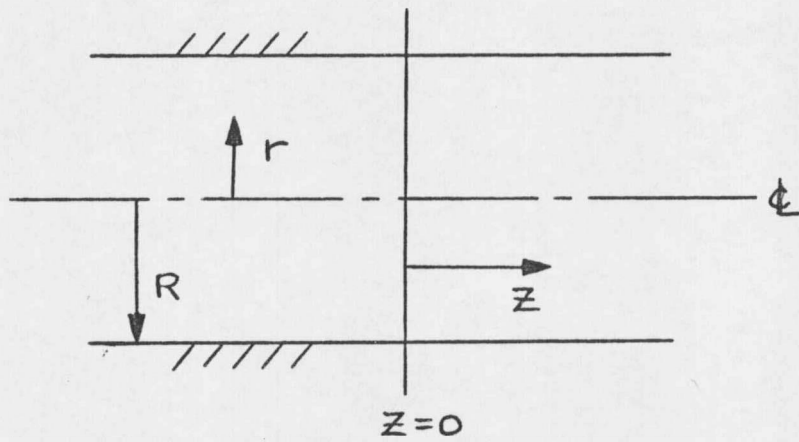


FIGURE 2. Axial Section of Pipe at an Arbitrarily Selected $z=0$ Position.

Equations (2.12), (2.13) and (2.14) are the theoretical expressions which imply the existence of a radial pressure gradient. Although it could be argued that the integral involving $\overline{v^2}$ and $\overline{w^2}$ is zero, the experimental data of Laufer [10], Gow [12], and others indicate that \overline{w} is always greater than \overline{v} except near the pipe centerline where they are equal. If \overline{w} is indeed greater than or at least equal to \overline{v} then equation (2.14) is always positive, which implies that the mean static pressure at the wall is greater than the mean static pressure at the centerline.

Equations (2.12), (2.13) and (2.14) were used to calculate the predicted curves for the radial pressure gradient by using the empirical data of Laufer [10] for values of $\overline{v^2}$ and $\overline{w^2}$.

CHAPTER III

LITERATURE REVIEW

A search of the literature was made to determine if any previous work had been done to measure experimentally the radial pressure gradient. That literature which was found included several technical papers and textbooks by Hinze [1], Schlichting [2], Longwell [3], and Pai [4].

The first source referred to was the ASME Codes [13]. These codes were reviewed in order to see what standards had been developed for the design of pitot-static probes or other applicable pressure measuring devices. This search revealed only one significant point which was that the static holes in the probe should be located at least eight support rod diameters upstream from the support rod. This length is sufficient to escape the effects of flow around a cylinder which could distort the true static pressure.

Regarding other applicable pressure measuring devices, Glaser [5] and Fechheimer [6] investigated two different types of pitot cylinders. Both of these designs utilized two holes located at a "critical angle" relative to one another. This "critical angle" is the angle at which the pressure distribution around a cylinder passes through the free stream static pressure value. However, the "critical angle" was different for each of the cases reported. In addition one can easily

show that the angle at which true static pressure occurs is a function of Reynolds number.

In 1959 R. Shaw [7] reported the influence of hole dimensions on static pressure measurements. His report stated that static pressure is influenced by the dimensions of a static pressure hole, and that an infinitely small hole would give the exact reading. A plot of pressure error (relative to a 0.0635 inch diameter reference hole) versus diameter of the static hole in inches was given for various average mean pipe velocities. The plots were extrapolated to zero diameter hole size and showed that the static holes of 0.0135 inches in diameter would give negligible error if no other contributing factors were present. The other factors included burrs around the outside and inside of the holes and deformed holes due to improper drilling.

Pai [8] presented a paper on turbulent flow in pipes in which he derived equation (2.14) for the radial pressure gradient. However, Pai's interpretation of the expression is different from this author's. Pai stated that the mean static pressure in the fluid will be greater than or equal to the mean static pressure on the wall for turbulent flow in circular pipes. The expression developed in this thesis is the same expression which Pai developed and existing data on turbulent flow indicates that the mean static pressure on the wall is greater than the mean static pressure in the fluid. It is not obvious how Pai

interpreted this expression.

In a paper by Brighton and Jones [9] the same expression (equation (2.14)) was derived for the radial pressure gradient. Their study was concerned with turbulent flow in annuli and they too interpreted the mean static pressure on the wall to be greater than the mean pressure in the fluid. However, they could not verify their theoretical results by experiment.

Laufer [10] has also reported on the structure of turbulence in fully developed pipe flow. In his paper he presented graphs of dimensionless fluctuating velocity components versus dimensionless radial position. These plots were for Reynolds numbers of 50,000 and 500,000 and showed no dependence of \bar{v} and \bar{w} on Reynolds number from the center of the pipe to about two-thirds of the way to the wall. This information was used in the development of expressions for \bar{v} and \bar{w} used in this thesis. These expressions for \bar{v} and \bar{w} are developed in digital computer programs which are available at Montana State University.

CHAPTER IV

EXPERIMENTAL SYSTEM

Apparatus

The experimental system shown schematically in Figure 3 was used throughout the investigation. Air was discharged from the centrifugal fan into the entrance section through eighty feet of flexible duct. Flow rates were controlled by a variable restriction on the inlet side of the fan. The entrance section, Figure 2 of Gow [12], contained a baffle plate and a series of screens to filter the air and dampen turbulence from the fan and return line. In the transition section, the cross sectional area of the entrance section was reduced from a four foot by four foot section to match the test pipe diameter of one foot. Seventy feet of one foot diameter aluminum irrigation pipe was used to insure fully developed flow at the test section. Suspension with adjustable brackets allowed for alignment of the pipe. The test section consisted of a three foot length of the same aluminum pipe coupled to the test pipe by a collar. The test section contained a static pressure piezometer ring and the experimental probe. The probe was mounted in the test section so that it could be moved radially from the center of the pipe to the wall.

The experimental probe was specially designed for this application

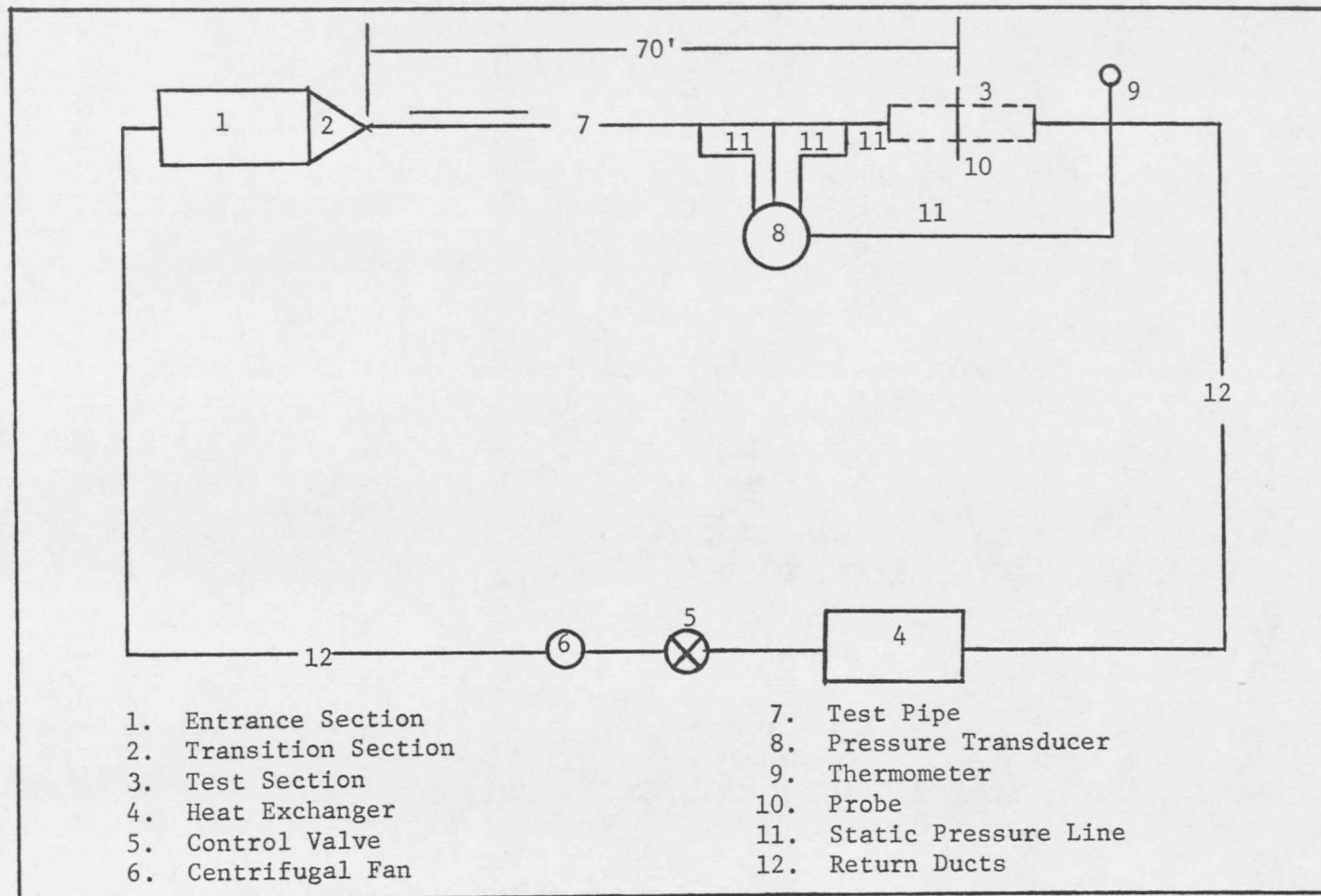


Figure 3. Schematic of Experimental System

Figure 4 illustrates the probe which consisted of a support rod running diametrically across the test pipe and two separate probes at 90° to the support rod and 180° from each other. The open-ended probe measured the total stagnation pressure. The closed-ended probe measured the normal stress of the fluid in a plane normal to the r direction. Unlike the standard pitot-static probe, the normal stress probe of this experiment had only two holes which opened into separate tubes connected to a differential pressure transducer. This arrangement allowed very precise alignment of the probe with the mean flow.

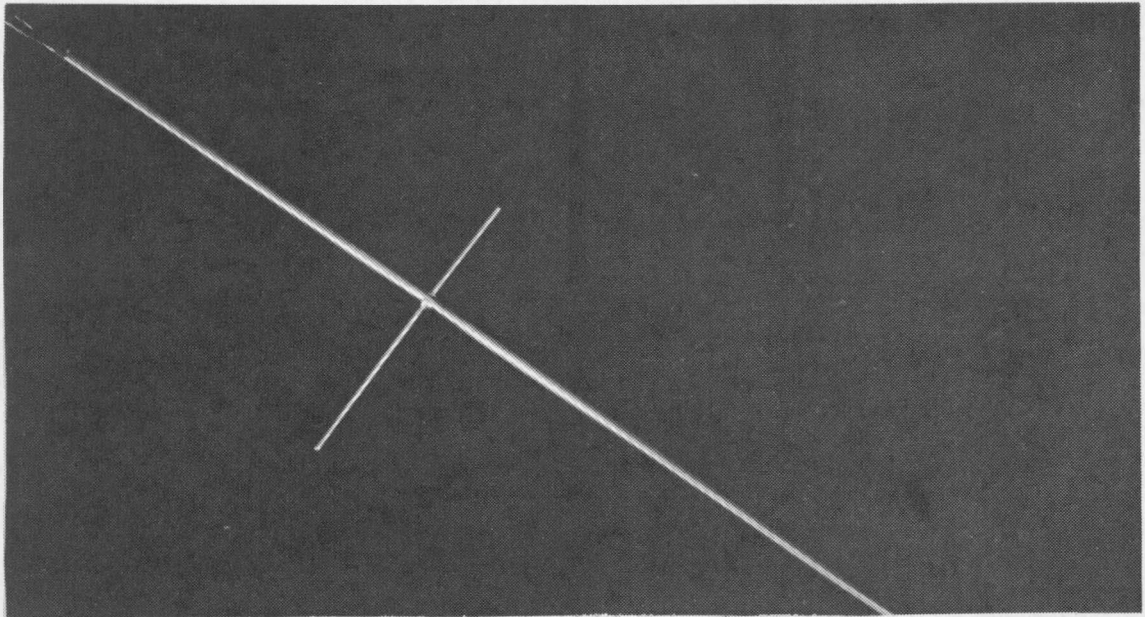
The normal stress which the probe measured is

$$\tau_{\theta\theta} = \bar{P} - \kappa \nabla \cdot \mathbf{U} + \rho \overline{w^2} \quad (2.15)$$

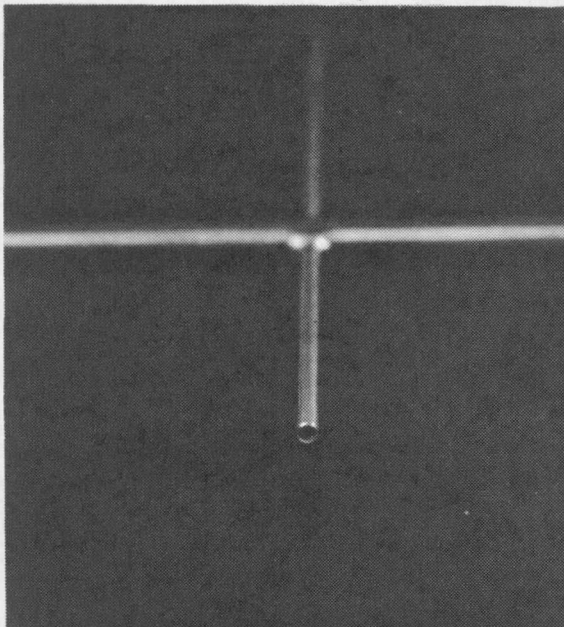
For incompressible flow the normal stress in the theta direction becomes

$$\tau_{\theta\theta} = \bar{P} + \rho \overline{w^2} \quad (2.16)$$

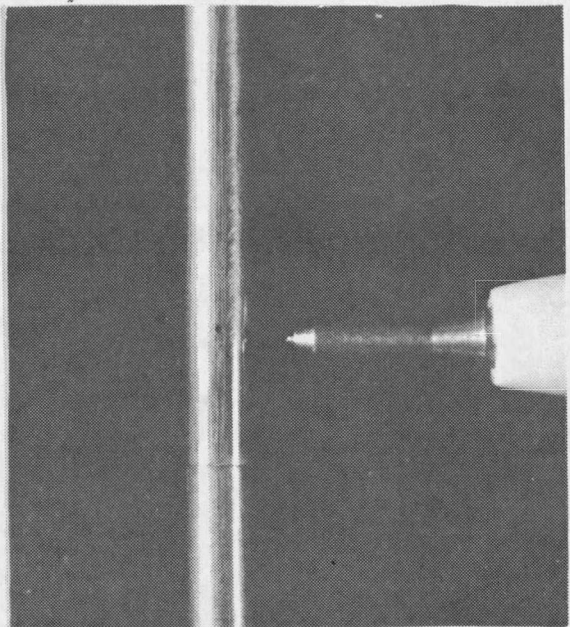
The turbulent fluctuating velocity component w is the only fluctuating velocity component which affects the measured stress. The component u is parallel to the probe and the component v is perpendicular to the probe. Therefore, these two components do not contribute to the indicated normal stress. From this point, the two parts of the probe will be referred to as the total head probe and the normal stress probe.



a) Overall view of probe



b) Total head probe



c) Normal stress probe

Figure 4. Final Probe Design

After measuring the normal stress of the fluid in the theta direction as discussed previously the mean static pressure, \bar{P} , could be calculated from equation (2.16). The quantity $\overline{\rho w^2}$ was calculated from an expression developed by Powe [11] for a Reynolds number of 165,000. The range of Reynolds numbers was extended from 50,000 to 500,000 by using a linear interpolating scheme applied to the v and w data of Laufer [10]. This procedure yielded an expression for w as a function of Reynolds number and radial position thus allowing the mean static pressure to be calculated from equation (2.16).

At several axial locations, four static pressure taps were mounted 90° apart around the circumference of the test pipe. The taps were connected in parallel to a taut diaphragm differential pressure transducer used to measure the static pressure drop in the test pipe. Thus, the static pressure read at each axial location was the average pressure of the four taps.

All pressure lines and the line from the normal-stress probe were connected to a manifold. An M.K.S. Instruments, Inc. differential pressure transducer, with a range of ± 1.0 mm.hg. and a stated accuracy of .00005 mm.hg. was used to measure the pressure differences between any two lines. For the larger Reynolds numbers, the measurements of dynamic head and absolute pressure measurements were made with a Meriam water manometer. The full range of the manometer was ± 20 inches of water with an accuracy of 0.001 inches of water.

The output of the differential pressure transducer was averaged and input to a Hickock Digital Voltmeter for monitoring. The reading on the meter was, depending on the scale setting of the transducer, then directly proportional to or equal to the actual pressure difference.

The air in the system was kept at a relatively constant temperature ($\pm .75^\circ$) by circulating water through two automobile radiators used as heat exchangers. The temperature of the air in the system was monitored using a conventional partial immersion mercury thermometer.

As illustrated in Figure 3 the system was made a closed system by connecting various pieces of apparatus with flexible ducting. A closed system was preferable in order to keep sand and dust particles out of the probes.

Appendix I contains a complete listing of equipment specifications and dimensions.

Procedure

As shown in Figure 4, the experimental probe was mounted across the pipe diametrically such that the total probe or the normal stress probe could be positioned directly upstream. A pointer was fixed to one end of the probe and an engineer's scale was mounted adjacent to the pointer. By moving the probe all the way into the wall and

knowing the pipe radius and probe radius the probe could be positioned in the center of the pipe to within $\pm .01$ inch. The probe could be rotated about its radial axis so that either the total probe or the normal stress probe could be used. After positioning the probe in the center of the pipe, the support rod was rotated until the total head probe was pointing upstream.

The first step of the actual experimental procedure was to measure the atmospheric pressure and temperature. Then the total probe was aligned directly into the flow by connecting one side of the manometer to the total head probe pressure line and connecting the other side of the manometer to the static wall tap at the same axial location as the probe. Rotation of the total probe to the position of highest deflection on the manometer assured reasonable alignment of the total probe with the flow and provided a value for the dynamic head. Next, by connecting one side of the manometer to atmosphere and the other side to the static wall tap at the test section, the static-atmospheric pressure difference could be measured. At this time the water temperature in the manometer was recorded. The pressure drops along the pipe were measured using the differential pressure transducer. All measurements previous to this statement were again taken at the end of a run to compare initial and final conditions.

Since the object of this study was to measure the difference in

static pressure from various radial positions to the wall, the probe had to be rotated so that the normal stress probe pointed upstream. This was done by initially rotating the probe until the pointer came in contact with the scale. Then by connecting each of the two taps in the normal stress probe to opposite sides of the differential pressure transducer, the difference in normal stress readings between each of the diametrically opposed taps could be made negligible by rotating the probe. Making the pressure difference between diametrically opposed taps essentially zero assured that the normal stress measured at each of the holes was the same and consequently that the probe was aligned parallel to the mean flow. Next, one of the lines from the normal stress probe was closed and the static wall tap at the axial location of the probe was opened to the other side of the transducer. The resulting difference in the radial pressure was then the pressure at the wall minus the normal stress in the theta direction measured by the normal stress probe. As was pointed out in the analytical development of Chapter II, the normal stress measured by the normal stress probe could be converted to static pressure using $\frac{w^2}{2}$ measurements.

When a reading was made at one radial position, the probe was then moved to the next radial position and the same method of zeroing and measuring was employed. This procedure was continued from the

center of the pipe to the wall. From the wall, the probe was moved directly to the center of the pipe and the static pressure at the wall minus the normal stress at the centerline was again checked. Also, a temperature reading of the system air was taken for each radial position. At this time the atmospheric pressure and temperature, the dynamic head, the static-atmospheric pressure and the axial pressure drops along the pipe were again recorded to determine if any changes had occurred during the data taking period.

This procedure was developed from the trial of three other experimental probes. The other probes tried were a standard pitot-static probe and two types of pitot-static cylinders. None of these probes worked reliably or accurately enough to justify their use. The probe and procedure finally adopted gave satisfactory results.

CHAPTER V

EXPERIMENTAL RESULTS

The results of the experimental data are presented in this section. Figures 5, 6, 7 and 8 are plots of dimensionless pressure difference and dimensionless normal stress difference versus dimensionless distance from the pipe wall. Figure 9 is a plot of dimensionless pressure difference and dimensionless normal stress difference from the wall to the centerline versus Reynolds number.

Figures 5, 6, 7, and 8 were obtained from the original experimental measurements of pressure differences using a digital computer program for the computations involved and for nondimensionalizing. The output of the data reduction program was used in plotting the pressure and normal stress gradients for ten different forms of nondimensionalizing. These ten forms were then carefully examined and the one which most clearly illustrated the results was chosen for presentation.

The computer programs used in this investigation are available at the Aerospace and Mechanical Engineering Department of Montana State University.

The accuracy of the experimental data when compared to the theoretical values indicates large percentage differences at all Reynolds numbers and at all radial positions.

Figure 5 illustrates the predicted and experimental curves for

the lowest Reynolds number (57,000) was used. The variation between predicted and experimental values of radial pressure difference is nearly constant from the wall to the centerline at this Reynolds number. The values of the experimental measurements are four to five times larger than the predicted values over the entire range of radial positions.

Figure 6 illustrates the predicted and experimental curves for a Reynolds number of 162,000. This plot shows the same shapes and trends as did Figure 5, except for slightly larger differences between measured and predicted values.

Figures 7 and 8 illustrate the predicted and experimental curves for Reynolds numbers of 292,000 and 484,000 respectively. These figures again show essentially the same information as did Figures 5 and 6. The differences being in the larger differences between measured and predicted values, up to ten to thirteen times, and the occurrence of the largest difference very near the wall.

Overall, Figures 5-8 show little agreement between predicted and experimental values of static pressure difference. However, the same general shape of radial static pressure gradient is illustrated in each plot. The greatest amount of radial pressure gradient occurs quite near the wall ($0 \leq y/R \leq .05$) with only slight change in pressure in the center portion of the pipe. There is also a definite Reynolds number dependence in static pressure difference. The

magnitude of radial static pressure difference increases with increasing Reynolds number near the wall and for all radial positions out to the center of the pipe.

As stated previously, Figure 9 is a plot of dimensionless pressure difference and dimensionless normal stress difference from the pipe wall to the centerline versus Reynolds number. Figure 9 shows a Reynolds number dependence in the value of static pressure at the wall minus static pressure at the centerline. The magnitude of the static pressure difference increases as the Reynolds number increases. This increasing trend is in agreement with the results of Figures 5-8. However, the large differences between experimental and predicted values cannot be explained completely for any of the Figures 5-9.

Some possible reasons for these large differences are:

1. Perhaps the probe did not measure the quantities for which it was designed.
2. Perhaps the lack of knowledge as to how v and w vary near the wall introduced error.
3. Hinze [1] states that incorrect pressure will be monitored if the measuring probe is of the same scale as the microscale of turbulence in which it is used, as was the case here.

Any or all of these factors could be present and affect the radial

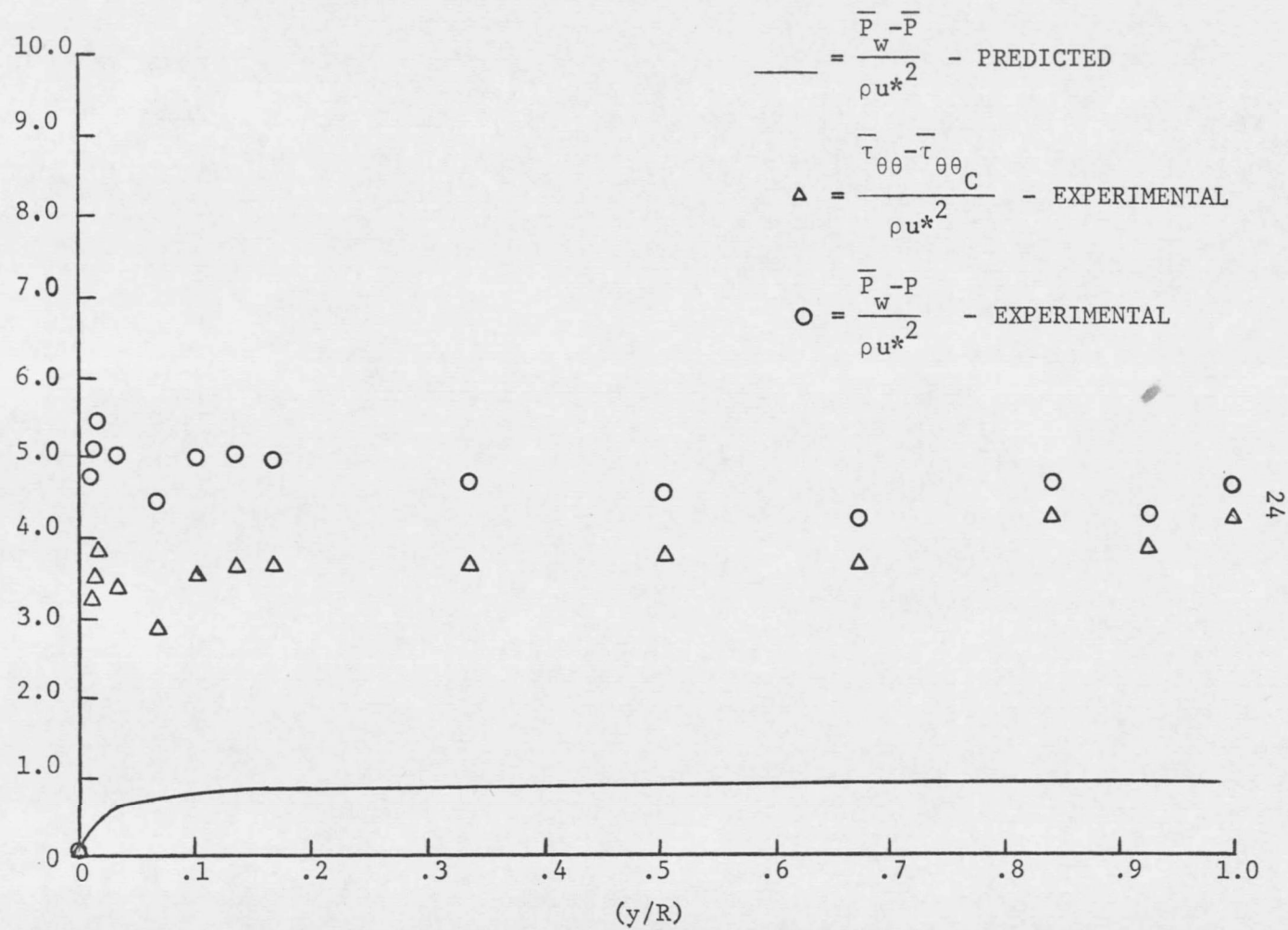


Figure 5. Normal Stress Difference at $Re = 57,000$

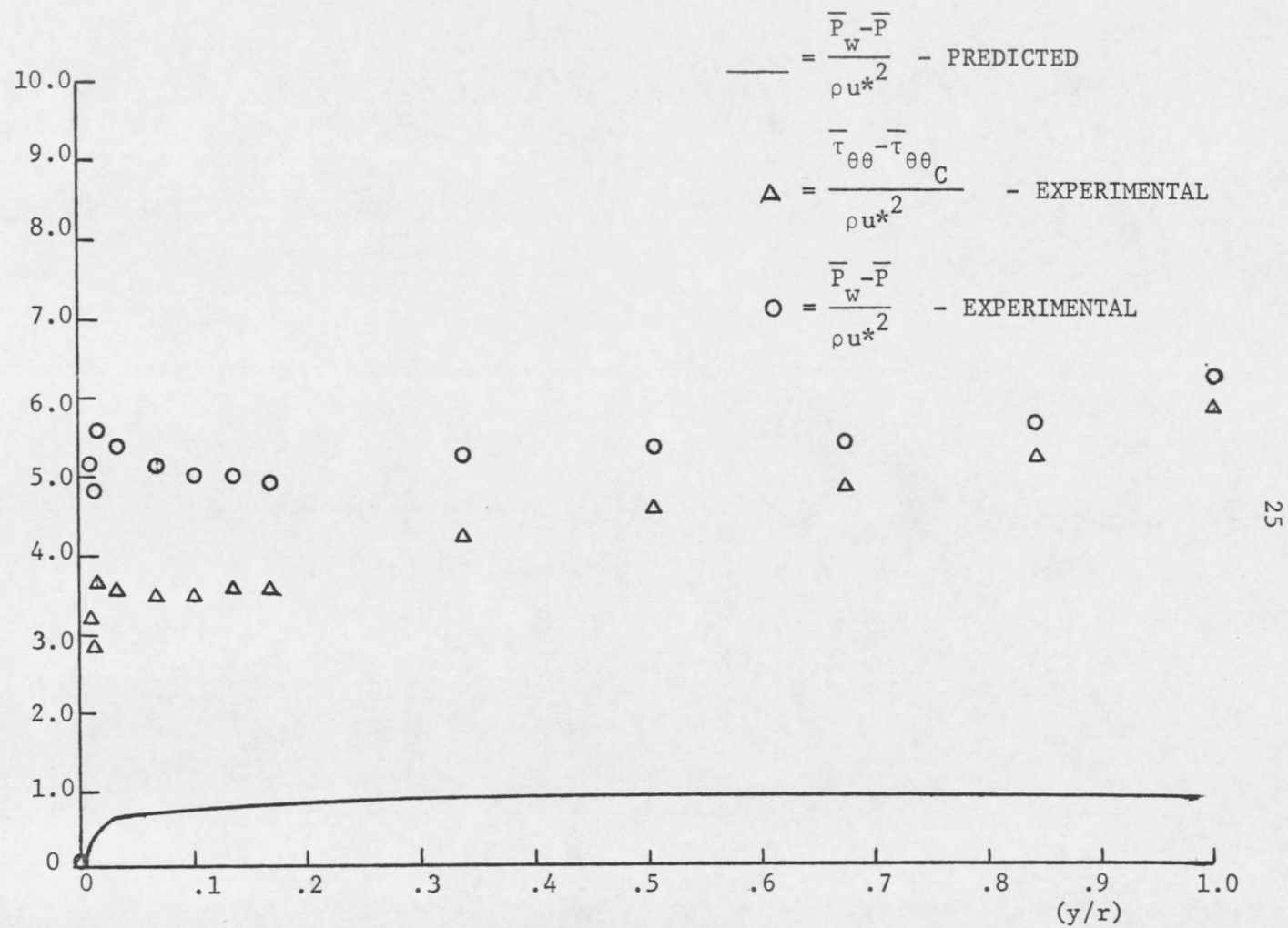


Figure 6. Normal Stress Differences at $Re = 162,000$

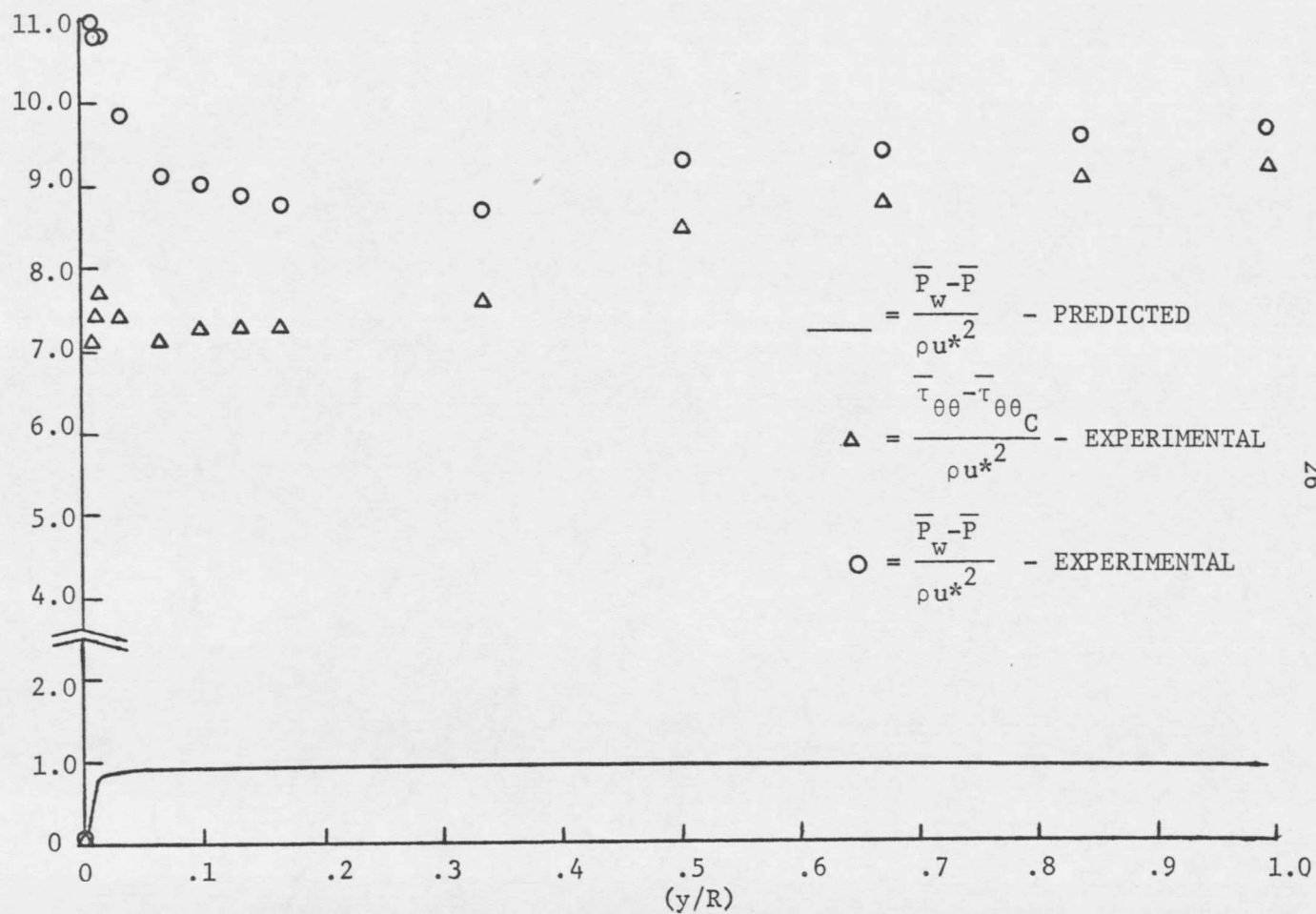


Figure 7. Normal Stress Differences at $Re = 292,000$

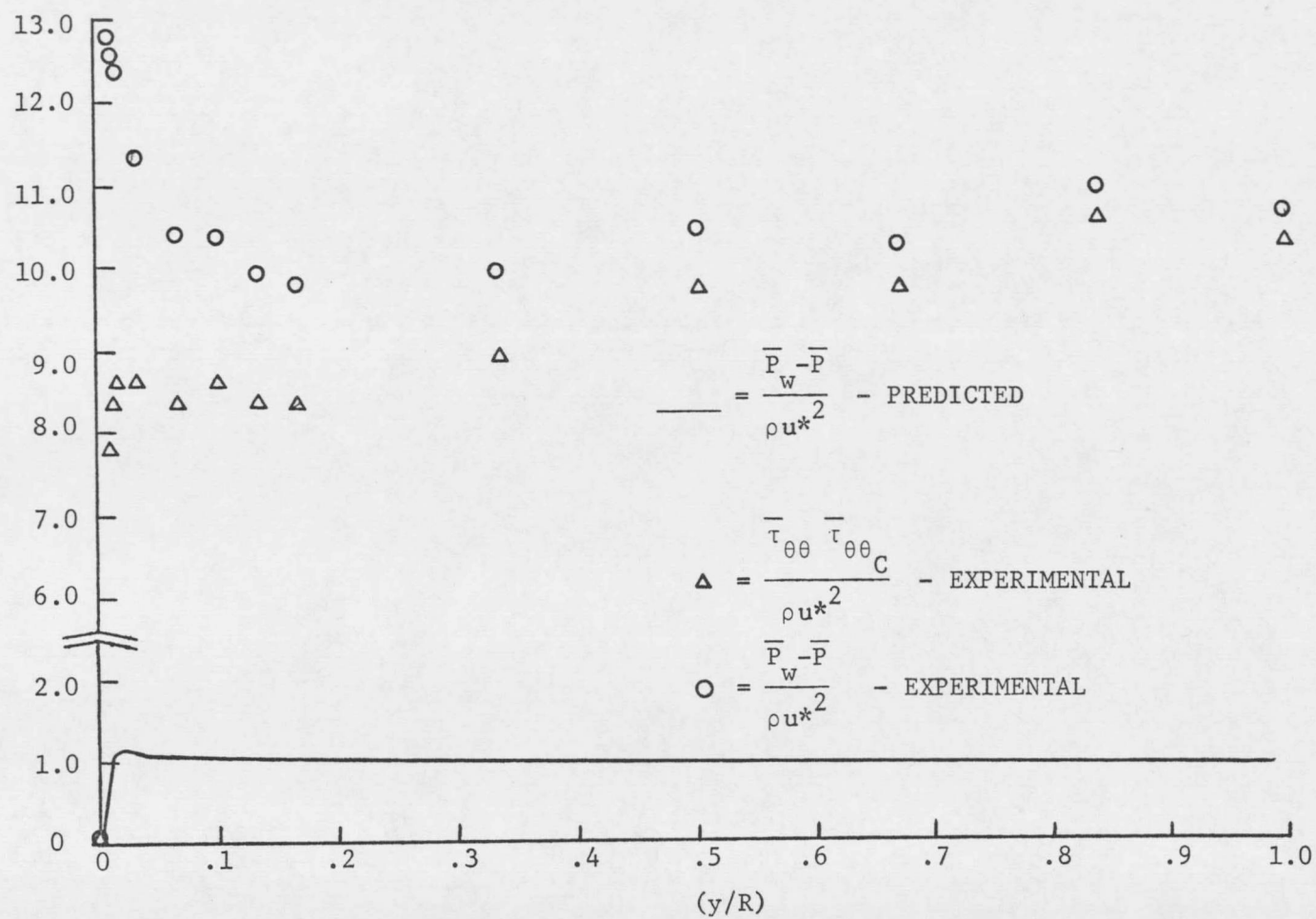


Figure 8. Normal Stress Differences at $Re = 484,000$.

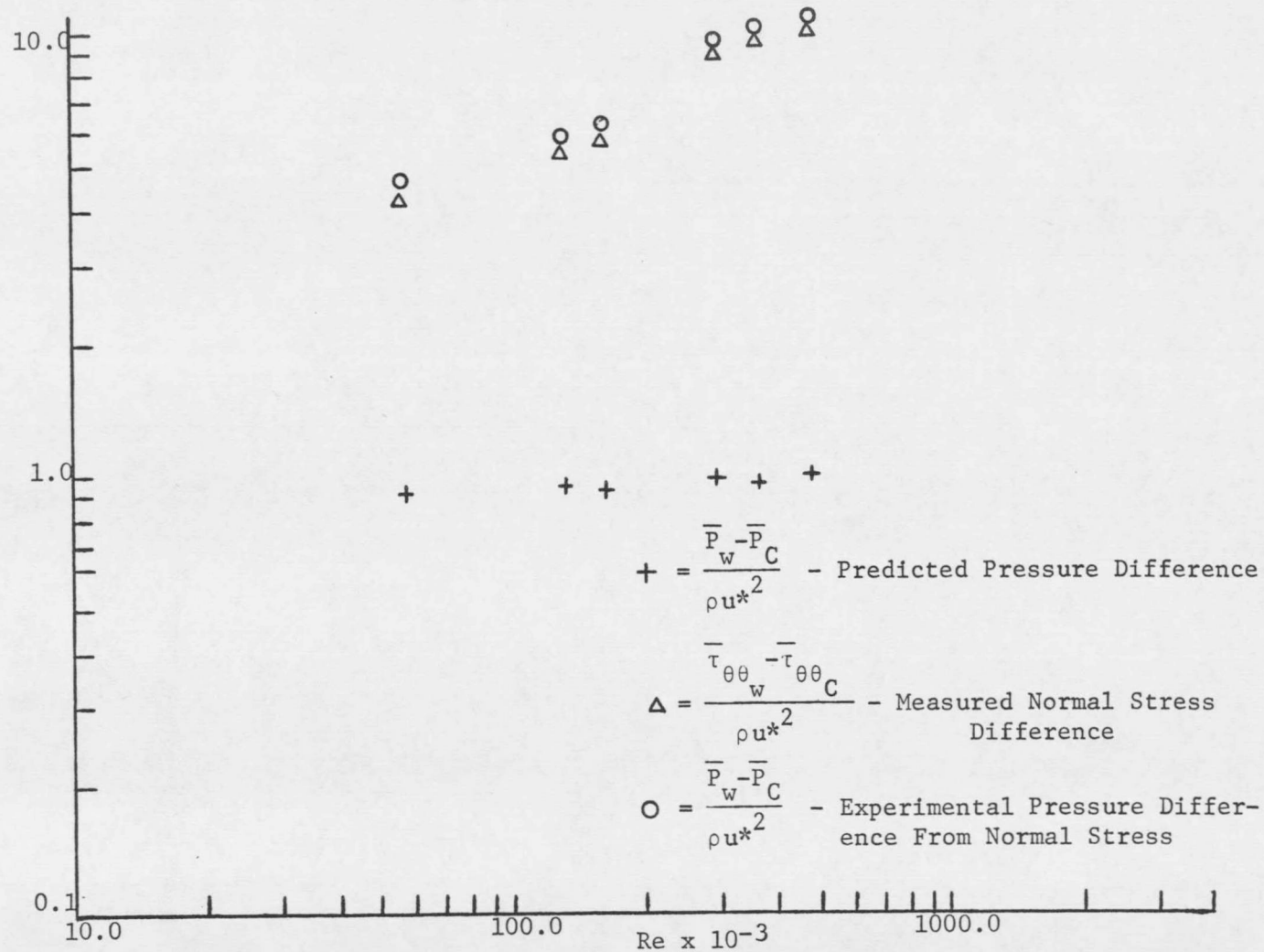


Figure 9. Dimensionless Normal Stress Differences Between Pipe Wall and Center Line as a Function of Reynolds Number

pressure difference values measured, but it is not obvious that any of these factors could contribute singly or any combination to produce the large differences observed between the measured and predicted pressure differences.

CHAPTER VI

CONCLUSION AND RECOMMENDATIONS

The existence of a static pressure gradient in the radial direction for turbulent flow through smooth walled pipes has been determined experimentally and compared with the theoretically predicted values.

In addition, it can be concluded that the magnitude of the radial pressure gradient is definitely a function of Reynolds number, the magnitude increasing as Reynolds number increases. Also, the shape of the pressure gradient varies with Reynolds number as can be seen in Figures 5-9.

It is recommended that this study be continued in flow through rough pipes. An interesting objective would be the determination of the changes in magnitude and shape of the pressure gradient resulting from the rough wall. Further studies in smooth pipes would probably not result in any new information. However, the use of a different type of pressure measuring device in smooth pipes could verify the results obtained in this study or perhaps result in experimental values which are closer to the predicted values.

APPENDIX I

EQUIPMENT SPECIFICATIONS

WIND TUNNEL EQUIPMENT

TEST PIPE

Aluminum irrigation pipe
Average radius - 5.94 inches
Standard deviation - 0.04 inches
Lengths - 15-20 feet

ENTRANCE SECTION

Filters, screens, and baffle plate
Cross-section reduced from 4 feet rectangular to circular
one-foot diameter in 7 feet as half sine wave.

MKS BARATRON TYPE 77 PRESSURE METER

Calibrated accuracy - 0.0005 mm Hg.
Type 77-H Pressure Head - diaphragm with capacitance sensor
Differential range - ± 1.1 mm Hg.
Type 77-MxR indicator null balancing - decade readout

HICKOCK D.C. DIGITAL VOLTMETER - MODEL DMS-3200

Voltage Range - 0- ± 1000 volts
Counter response - Pulse rates to 10^6 PPS
Dimensions - 9-1/4 in. w. x 6-3/8 in. l. x 12-7/8 in. d.


LITERATURE CITED

1. Hinze, J. O., Turbulence, McGraw-Hill Book Company, New York (1959).
2. Schlichting, H., Boundary Layer Theory, McGraw-Hill Book Company, New York, 6th Edition (1968).
3. Longwell, P. A., Mechanics of Fluid Flow, McGraw-Hill Book Company, New York (1966).
4. Pai, S. I., Viscous Flow Theory, I-Laminar Flow, Van Nostrand Co., Inc., Princeton, New Jersey (1956).
5. Glaser, A. H., "The Pitot Cylinder as a Static Pressure Probe in Turbulent Flow", Journal of Scientific Instruments, 29: (219) (1952).
6. Fechheimer, C. J., "Measurement of Static Pressure", Transactions of American Society of Mechanical Engineers, 48: (965) (1926).
7. Shaw, R., "The Influence of Hole Dimensions on Static Pressure Measurements", Journal of Fluid Mechanics, 7: 550 (1959).
8. Pai, S. I., "On Turbulent Flow in Circular Pipe", Journal of the Franklin Institute, 20: 337 (1953).
9. Brighton, J. A. and J. B. Jones, "Fully Developed Turbulent Flow in Annuli", Journal of Basic Engineering, 835 (1964).
10. Laufer, John, "The Structure of Turbulence in Fully Developed Pipe Flow", NACA Report 1174, (1954).
11. Powe, R. E., "Turbulence Structure In Smooth and Rough Pipes", Ph.D. Thesis, Aerospace and Mechanical Engineering, Montana State University, Bozeman, (1970).
12. Gow, J. L., "Fully-Developed Turbulent Flow In Smooth and Rough-Walled Pipe", M.S. Thesis, Aerospace and Mechanical Engineering, Montana State University, Bozeman (1969).

MONTANA STATE UNIVERSITY LIBRARIES



3 1762 10013911 0


M378
G829
Cop. 2

X